Organic Process Research & Development **2009**, *13*, 1343–1356

Seeded Batch Cooling Crystallization with Temperature Cycling for the Control of Size Uniformity and Polymorphic Purity of Sulfathiazole Crystals

Mohd R. Abu Bakar, Zoltan K. Nagy,* and Chris D. Rielly

Department of Chemical Engineering, Loughborough University, Loughborough, Leicestershire LE11 3TU, United Kingdom

Abstract:

An experimental study has been conducted to evaluate the capability of a seeded batch cooling crystallization with a temperature cycling method to produce a narrow crystal size distribution and grow a desired polymorphic form of sulfathiazole crystals. The study used focused beam reflectance measurement (FBRM), and attenuated total reflectance ultraviolet/visible (ATR-UV/vis) spectroscopy for the *in situ* monitoring and control of the process. Based on the FBRM readings, the process was driven using a feedback control approach that employs alternating cycles of heating and cooling phases so that the number of counts, corresponding to the number of seed particles, is maintained, whilst the square-weighted chord length distribution, indicating the dynamic progress of the growth of the seeds in the system, is increased. Results of the experiments show that the temperature cycling method promoted Ostwald ripening, which helped in accelerating the growth and enhancing the size uniformity of the product. The method also has a good prospect to be implemented for the control of polymorphic purity. Seeds of Form I and Form II could be grown from *n*-propanol and water, respectively. Form I seeds in water were first transformed into Form II and/or swamped by nuclei of Form II, before the growth of the newly formed crystals took place. Seeds of Form II and Form III in *n*-propanol, however, were not able to grow at all. This study confirmed that the nucleation and growth of sulfathiazole crystals are solvent-mediated, and the insight into these phenomena was captured very well by the *in situ* monitoring tools.

1. Introduction

Crystallization is an important unit operation used in many chemical process or pharmaceutical industries. The objective of the operation is to generate crystals with desired qualities including crystal size distribution (CSD), habit, purity and polymorphic form. In order to achieve this objective, a careful selection of the crystallization operation and control method is required. The application of process analytical tools has led to novel control approaches for pharmaceutical crystallization, which can yield significant product quality improvements. Alongside supersaturation control[1−9] and, more recently, a direct nucleation control,[10] the method of seeding also plays an important role in defining the properties of the crystals produced. Seeding is widely used in the control of CSD[11−15] and has been successfully applied in the control of polymorphism.[16−18] Generally, the technique involves the introduction of seed crystals in a supersaturated solution, and the operating curve afterward should remain within the metastable zone.[19,20] During the process, secondary nucleation is expected to take place, and the supersaturation is mainly used for the growth of seeds. This type of seeding technique circumvents the uncertainties in the spontaneous primary nucleation since the system is not allowed to become labile.[6]

Seed crystals can be generated either directly from recrystallization or from subsequent particle-size reduction processes including sifting, screening, sonication, supercritical fluid extraction and particle-size reduction followed by ripening (ageing). These processes, however, may not eliminate, and may even promote, the uncertainty in the size uniformity of the produced seed crystals. Seed crystals can also be present as mixtures of polymorphs, since many polymorphic systems tend to crystallize in mixtures.[21] The polymorphic purity of the seed crystals is crucial, especially if production of a certain pure form is desired.[22] Recently, several innovative approaches have been proposed to control the formation of a particular polymorphic form on the basis of supersaturation control[19,20] or model-based

* Author for correspondence. Telephone: + 44 (0)1509 222 516. Fax: + 44 (0)1509 223 953. E-mail: Z.K.Nagy@lboro.ac.uk.

(1) Braatz, R. D. *Ann. Rev.Control* **2002**, *26*, 87–99.
(2) Larsen, P. A.; Patience, D. B.; Rawlings, J. B. *IEEE Control Syst. Mag.* **2006**, *26*, 70–80.
(3) Worlitschek, J.; Mazzotti, M. *Cryst. Growth Des.* **2004**, *4*, 891–903.
(4) Gron, H.; Borissova, A.; Roberts, K. J. *Ind. Eng. Chem. Res.* **2003**, *42*, 198–206.
(5) Nonoyama, N.; Hanaki, K.; Yabuki, Y. *Org. Process Res. Dev.* **2006**, *10*, 727–732.
(6) Yu, Z. Q.; Chow, P. S.; Tan, R. B. H. *Ind. Eng. Chem. Res.* **2006**, *45*, 438–444.
(7) Fujiwara, M.; Nagy, Z. K.; Chew, J. W.; Braatz, R. D. *J. Process Control* **2005**, *15*, 493–504.
(8) Zhou, G. X.; Fujiwara, M.; Woo, X. Y.; Rusli, E.; Tung, H.; Starbuck, C.; Davidson, O.; Ge, Z.; Braatz, R. D. *Cryst. Growth Des.* **2006**, *6*, 892–898.
(9) Nagy, Z. K.; Chew, J. W.; Fujiwara, M.; Braatz, R. D. *J. Process Control* **2008**, *18*, 399–407.
(10) Abu Bakar, M. R.; Nagy, Z. K.; Saleemi, A. N.; Rielly, C. D. *Cryst. Growth Des.* **2009**, *9* (3), 1378–1384.
(11) Patience, D. B.; Dell'Orco, P. C.; Rawlings, J. B. *Org. Process Res. Dev.* **2004**, *8* (4), 609–615.
(12) Warstat, A.; Ulrich, J. *Chem. Eng. Technol.* **2006**, *29* (2), 187–190.
(13) Yu, Z. Q.; Chow, P. S.; Tan, R. B. H. *Org. Process Res. Dev.* **2006**, *10* (4), 717–722.
(14) Kubota, N.; Noihito, D. *Powder Technol.* **2001**, *121* (1), 31–38.
(15) Loi Mi Lung-Somarribaa, B.; Moscosa-Santillanb, M.; Portea, C.; Delacroix, A. *J. Cryst. Growth* **2004**, *270*, 624–632.
(16) Beckmann, W.; Otto, W.; Budde, U. *Org. Process Res. Dev.* **2001**, *5* (4), 387–392.
(17) Beckmann, W. *Org. Process Res. Dev.* **2000**, *4* (5), 372–383.
(18) Beckmann, W.; Nickisch, K.; Budde, U. *Org. Process Res. Dev.* **1998**, *2* (5), 298–304.
(19) Kee, N. C. S.; Arendt, P. D.; Tan, R. B. H.; Braatz, R. D. *Cryst. Growth Des.* **2009**, *9*, 3052–3061.
(20) Kee, N. C. S.; Tan, R. B. H.; Braatz, R. D. *Cryst. Growth Des.* **2009**, *9*, 3044–3051.
(21) Abu Bakar, M. R.; Nagy, Z. K.; Rielly, C. D. *J. Therm. Anal. Calorim.* **2009**. In press
(22) Mller, M; Meier, U.; Wieckhusen, D.; Beck, R.; Pfeffer-Hennig, S.; Schneeberger, R. *Cryst. Growth Des.* **2006**, *6* (4), 946–954.

10.1021/op900174b CCC: $40.75
Published on Web 11/03/2009

control approaches.[23−25] However, in practice often it is difficult to guarantee the polymorphic purity and the quality of the seed size distribution. In these cases it is possible to correct the quality of the seed crystals *in situ* and consequently improve the quality of the product by applying alternating cycles of heating and cooling phases. These temperature fluctuations increase the kinetics of Ostwald ripening[26] since the dissolution of fine particles (and/or unwanted polymorphic forms) is accelerated during heating phases, while the growth of the larger crystals is accelerated during cooling phases. This temperature fluctuations method, known as the temperature cycling method, was previously proposed by Carless and Foster[27] to accelerate crystal growth. A similar method was also proposed by Loi Mi Lung-Somarribaa and co-workers[15] to control the CSD.

In this report a seeded batch crystallization with the temperature cycling method will be studied with the objective of simultaneously controlling the CSD and the polymorphic purity of sulfathiazole crystals. Extensive studies have been carried out which demonstrate the importance of process analytical tools for the detection or control of polymorphic transformations.[28−30] In this work, a Lasentec focused beam reflectance measurement (FBRM) was used for *in situ* detection and monitoring of unwanted primary nucleation, dissolution of fine particles and growth evolution of the seed crystals, whilst attenuated total reflectance ultraviolet−visible spectroscopy (ATR UV−vis) was utilized for *in situ* and in-process monitoring of the solute concentration in the system. FBRM has been widely used for monitoring crystallization processes. Although it cannot provide direct information about nucleation and crystal growth, the evolution of the newly formed particles (after nucleation and growth to the detectable size) and the chord length distribution give valuable information, which can be indirectly related to the nucleation, growth, agglomeration or attrition phenomena during the crystallisation process.[31]

The model system, sulfathiazole, presently has five known polymorphs that are well characterized in the literature.[32] There are some inconsistencies in the enumeration of the sulfathiazole polymorphs; in this work, the enumeration of the polymorphs follows the convention proposed by Apperley and coresearchers.[32] Previous studies have found that the crystallization of sulfathiazole polymorphs were dependent mainly on the solvent[33,34] for example, crystallizations from *n*-propanol were reported to consistently produce Form I only, whereas crystallizations from water were found to generate Form II and Form III.[33]

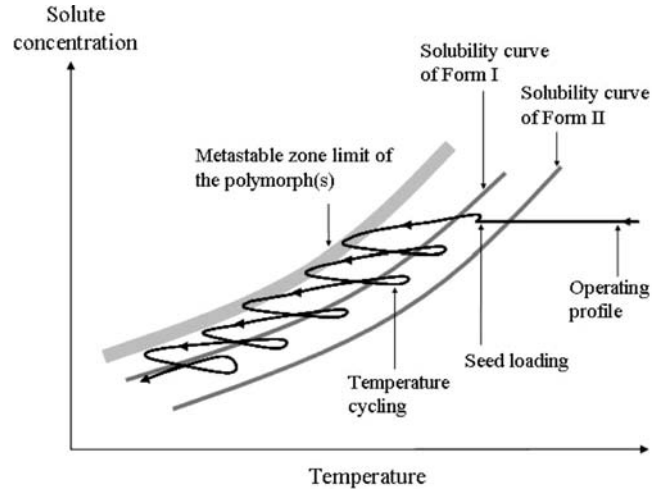

Figure 1. **The hypothetical operating profile of the proposed seeded batch crystallization with temperature cycling.**

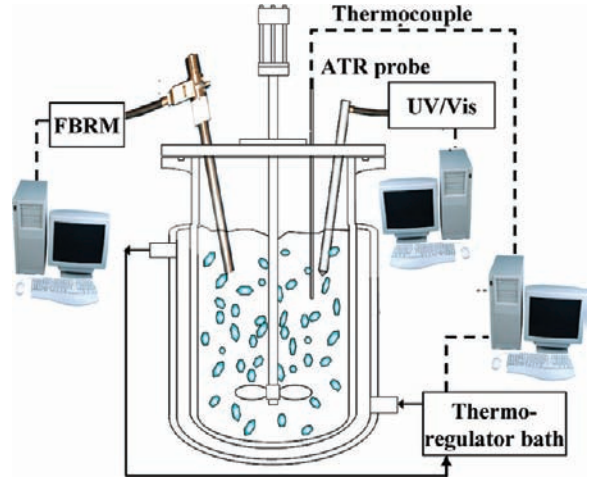

Figure 2. **Schematic representation of the experimental setup.**

Figure 1 shows hypothetically the operating profile of the proposed approach on a phase diagram of a monotropic system with two polymorphs, Form I and Form II. In this case, Form II is the desired polymorph, and the seed crystals are unsieved and contain both polymorphs. Once the seeds are loaded, it should be expected that some of the seeds of Form I will dissolve since the seed loading point lies in the undersaturated region of Form I. For this reason, the solute concentration is slightly increased during seed loading as depicted in Figure 1. In order to eliminate the presence of Form I as well as fine particles from the seed crystals, a temperature cycling method, which is a succession of heating and cooling phases, is applied after the seed loading. Ideally the operating profile should at all times lie below the solubility curve of Form I, but in the supersaturation region of Form II. However this is very difficult to achieve since most of the solubility curves of different polymorphs of a system are very close to each other. For this reason, the heating and cooling phases may cross the solubility curve of Form I, as shown in Figure 1. On cooling, the supersaturation is expected to be used for the growth of the

(23) Ono, T.; Kramer, H. J. M.; Ter Horst, J. H.; Jansens, P. J. *Cryst. Growth Des.* **2004**, *4*, 1161–1167.
(24) Hermanto, M. W.; Chiu, M.-S.; Woo, X. Y; Braatz, R. D. *AIChE J.* **2007**, *53*, 2643–2650.
(25) Hermanto, M. W.; Braatz, R. D.; Chiu, M.-S. *AIChE J.* **2009**, *55*, 122–131.
(26) Boistelle, R.; Astier, J. P. *J. Cryst. Growth* **1988**, *90*, 14–30.
(27) Carless, J. E.; Foster, A. A. *J. Pharm. Pharmacol.* **1966**, *18*, 697–708.
(28) Fevotte, G. *Int. J. Pharm.* **2002**, *241*, 263–278.
(29) Fevotte, G. *Chem. Eng. Res. Des.* **2007**, *85* (7), 906–920.
(30) Simon, L. L.; Nagy, Z. K.; Hungerbuehler, K. *Chem. Eng. Sci.* **2009**, *64*, 3344–3351.
(31) Nagy, Z. K.; Fujiwara, M.; Woo, X. Y.; Braatz, R. D. *Ind. Eng. Chem. Res.* **2008**, *47*, 1245–1252.
(32) Apperley, D. C.; Fletton, R. A.; Harris, R. K.; Lancaster, R. W.; Tavener, S.; Threlfall, T. L. *J. Pharm. Sci.* **1999**, *88*, 1275–1280.
(33) Khoshkhoo, S.; Anwar, J. *J. Phys. D: Appl. Phys.* **1993**, *26*, 890–893.
(34) Anderson, J. E.; Moore, S.; Tarczynski, F.; Walker, D. *Spectrochim. Acta, Part A* **2001**, *57*, 1793–1808.

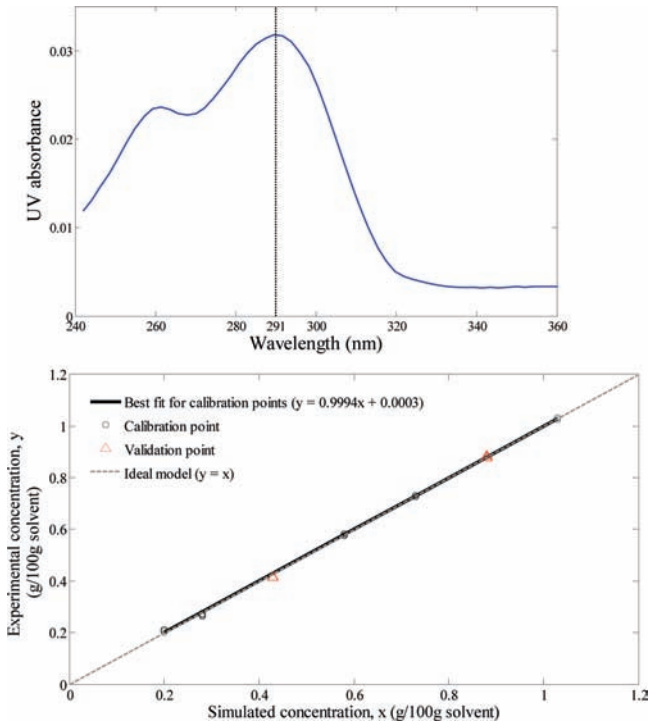

Figure 3. **Plots of (a) typical absorbance spectra of sulfathiazole in *n*-propanol in a range of 242−360 nm; and (b) experimental concentrations against simulated concentrations.**

seeds, and hence the profile of the cooling phases shows a decreasing trend in solute concentration. On heating, the fine particles and the unwanted polymorph are expected to dissolve, and hence the profile of the heating phases shows an increasing trend in solute concentration. The transition between heating and cooling phases creates loops, as shown in the figure. As can be seen in Figure 1, the temperature cycling is continued progressively stepping down towards a low temperature. This is to maintain the supersaturation in the system, so that the seed crystals can continuously grow. The crystallisation process should be stopped and the end product should be collected only when the profile lies in the undersaturated region of Form I but in the saturated region of Form II in order to ensure that no crystals of Form I are present in the product.

In this paper, experimental results from a seeded batch crystallization with temperature cycling method, implemented using sulfathiazole in *n*-propanol and in water as model systems, are presented and the capability of the method to produce uniform size crystals and to grow the desired polymorphic form is evaluated. The temperature cycling method can provide superior performance compared to supersaturation control based approaches, for cases when the seed has a broad CSD with a significant amount of fines, or when fines are formed during the crystallization process due to attrition (often observed in the case of crystals with needle morphology commonly encountered for pharmaceutical compounds). Also when the seed has unwanted polymorphic impurity of Form I, or the compound nucleates as mixtures of Form I and Form II, the temperature cycling method can be used to eliminate the unwanted Form I, enriching the system in Form II. For systems with very slow growth rates and when the desired form is the metastable polymorph, controlling the process at constant high supersaturation may induce secondary nucleation and hence generate unwanted fines and/or another polymorph. If the system is controlled at low supersaturation to avoid secondary nucleation, crystallization times will be excessively long and may lead to the transformation of the metastable form into the thermodynamically more stable form. For most pharmaceutical systems the solubility curves of the various polymorphs are very close, and operation within the narrow zone between the solubility curves using a supersaturation control approach may be impractical, due to the very low supersaturation or due to errors in concentration measurement or limitations in the cooling system. In these cases the temperature cycling method can provide a more practical approach, with superior performance compared to the constant supersaturation controlled processes. The conditions under which various polymorphic forms can grow in the system are also corroborated in this contribution via seeded temperature cycling experiments.

2. Experimental Section

2.1. Materials. Sulfathiazole was purchased from Sigma Aldrich with a purity of 98%. The solvents used were *n*-propanol (analytical reagent grade, Fisher Scientific), water (ultrapure, generated from a Milli-Q reversed osmosis unit) and ammonium hydroxide (analytical reagent grade, Fisher Scientific).

2.2. Apparatus. The crystallization experiments were performed in a jacketed 500 mL glass vessel. The temperature in the vessel was controlled with a PTFE thermocouple connected to a thermo fluid circulator bath (Huber Variostat CC-415 vpc). The temperature readings were recorded every 20 s on a computer by a control interface written in LabVIEW (National Instruments). An overhead stirrer with a PTFE three-bladed marine type impeller was used to agitate the system at 320 rpm. A focussed beam reflectance measurement (FBRM) probe (model D600, Lasentec) was inserted into the solution to measure chord length distributions. The distributions were collected every 20 s and averaged during collection. They were monitored using the FBRM control interface software (version 6.7). The UV system used was a Zeiss MCS621 spectrometer with a CLD600 lamp module. Absorbance spectra were obtained through a Hellma 661.822 Attenuated Total Reflectance (ATR) UV/vis probe, which was directly immersed in the solution. The spectral range was 242 − 360 nm, and a spectrum of the solution was recorded every 20 s using a data acquisition software, Aspect Plus (version 1.76). A schematic representation of the experimental setup is shown in Figure 2.

2.3. Solubility of Sulfathiazole in *n*-Propanol. The solubility of sulfathiazole in its raw form in *n*-propanol was determined using a gravimetric method, as described in the authors' previous work.[10] It was determined at temperatures ranging from 30 to 70 °C.

2.4. Calibration for Solution Concentration. Specified amounts of sulfathiazole and *n*-propanol were placed in a 500 mL jacketed glass vessel, and with the overhead stirrer agitating the system, the slurry was heated to about 10 °C above its saturation temperature. The slurry was kept at this elevated temperature for at least 20 min to ensure all crystals had dissolved. The clear solution was then subjected to a negative step change of 5 °C and was left to equilibrate at the set temperature for 10 min. The procedure was continued for five

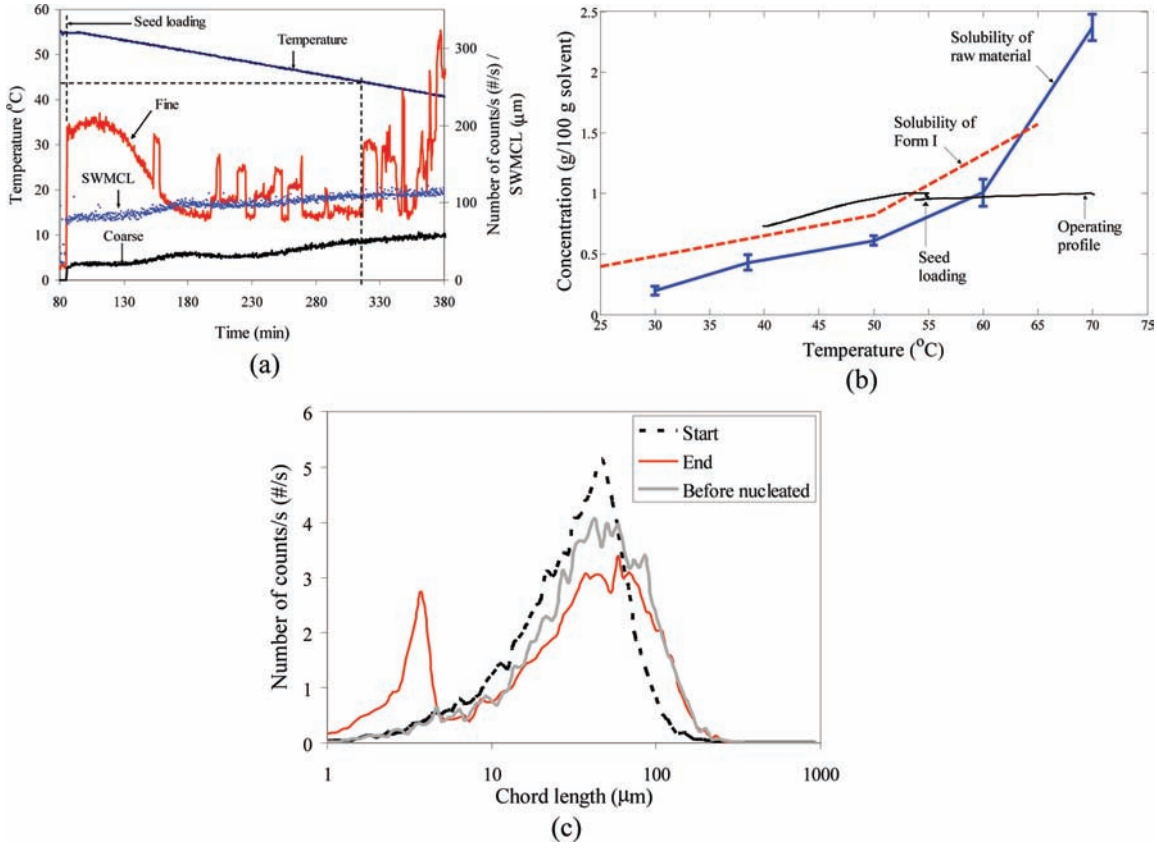

Figure 4. **Profiles of (a) temperature, number of fine and coarse, and SWMCL; (b) solution concentration on the phase diagram; and (c) CLDs at the start, the end and before the nucleation of the seeded batch crystallization of Form I in *n*-propanol with linear cooling.**

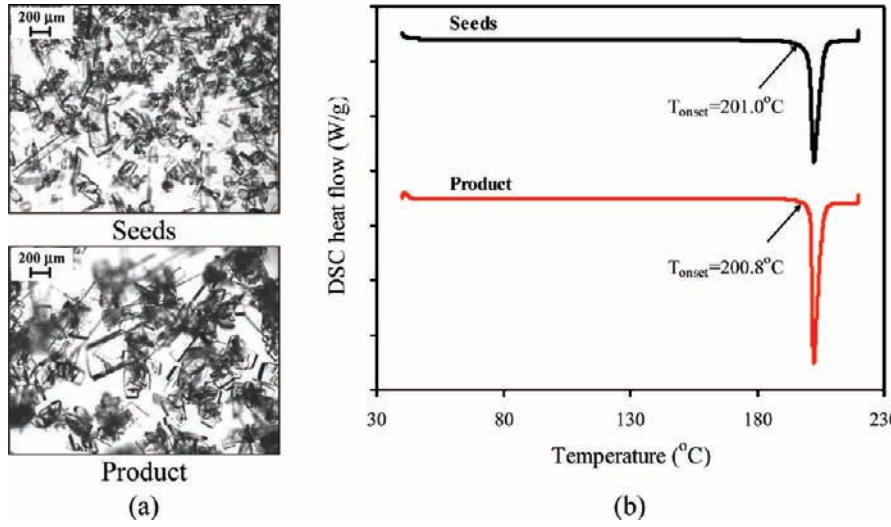

Figure 5. **(a) Microscopy images and (b) DSC curves of the seeds and product of the seeded batch crystallization of Form I in *n*-propanol with linear cooling.**

other different set temperatures or until the FBRM detected a nucleation event. In the latter case, the system was brought back to dissolution by heating, and then the negative step change procedure was repeated down to a temperature slightly above the nucleation point. In order to take into account the hysteresis effect between cooling and heating runs on the absorbance spectra measurement, the solution was subsequently subjected to a positive step change to repeat the measurement at all set temperatures. Once the cooling−heating cycle was completed, a specific amount of sulfathiazole was added to the solution to change the solution concentration, and the procedure was repeated, stepping up to progressively higher concentration systems. Stepping up instead of stepping down of the system concentration was performed because, throughout the experiment, the solvent needs to be kept at the vessel's maximum capacity in order to prevent the formation of crust on the vessel wall. For calibration purposes, absorbance spectra were collected for six different solution concentrations ranging from 0.20 to 1.03 g per 100 g propan-1-ol, over temperatures in the range from 20 to 65 °C.

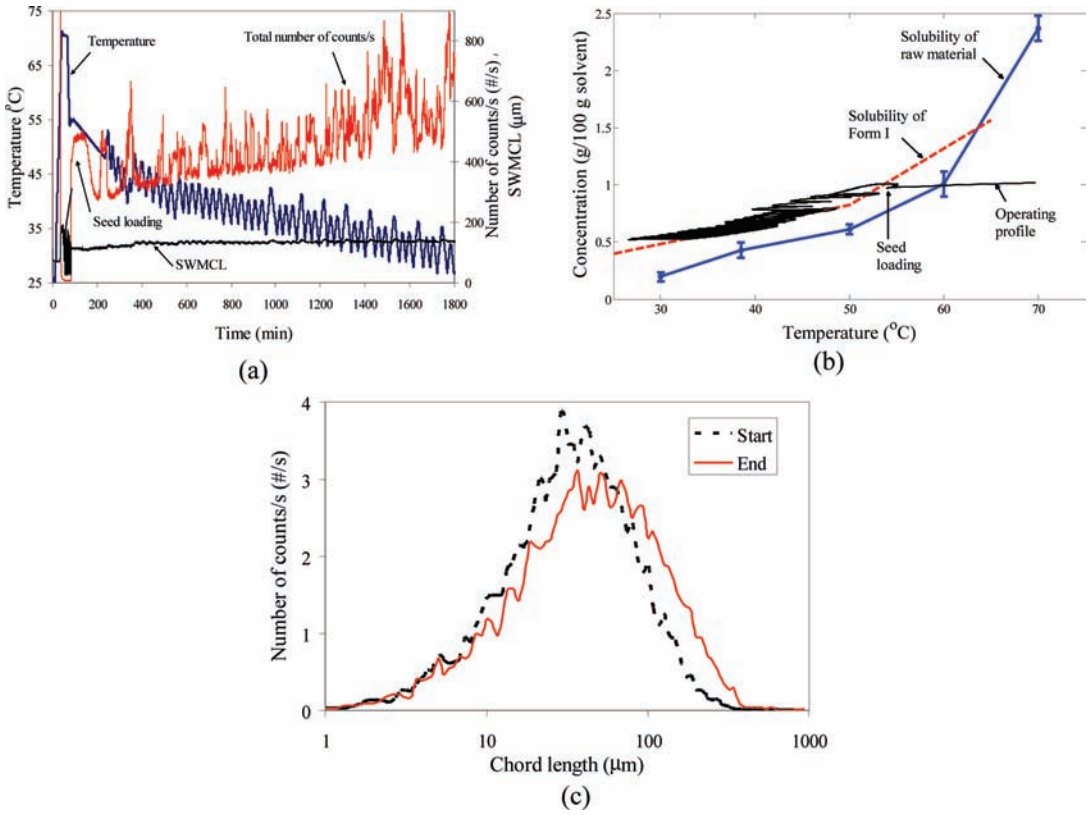

Figure 6. **Profiles of (a) temperature, total number of counts/s and SWMCL; (b) solution concentration on the phase diagram; and (c) CLD at the start and the end of the seeded batch crystallization of Form I in *n*-propanol with temperature cycling.**

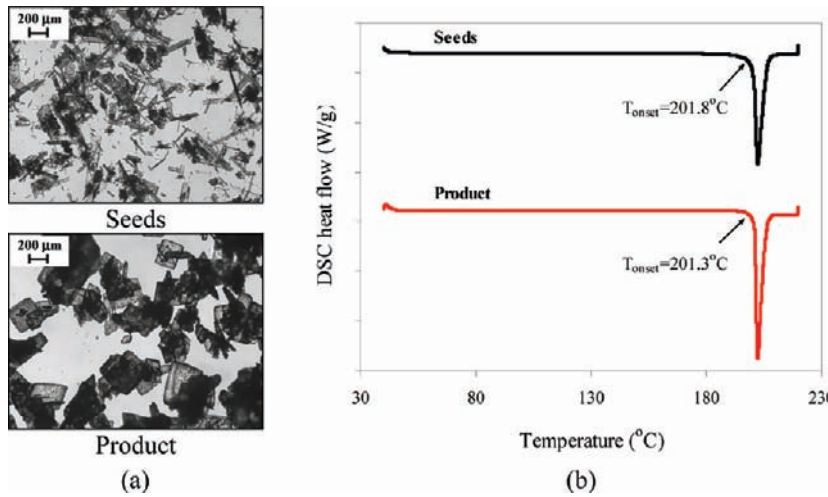

Figure 7. **(a) Microscopy images and (b) DSC curves of the seeds and product of the seeded batch of Form I in *n*-propanol with temperature cycling.**

2.5. Preparation of Seeds. Sulfathiazole crystals of different polymorphs for seed were prepared using methods based on those available in the literature. Form I was prepared by heating a saturated *n*-propanol solution at 80 °C (7.2 g of sulfathiazole in 300 g of *n*-propanol) in the crystallization vessel to dissolution, followed by natural cooling to 20 °C.[33,35] Form II was generated by rapid cooling of an aqueous solution of sulfathiazole (6.0 g of sulfathiazole in 600 g of water) from 80 to 4 °C.[33] Form III was prepared by slow evaporation of ammonium hydroxide solution at room temperature.[35] All of the obtained crystals were vacuum filtered, and subsequently, the crystals prepared from water were immediately dried in a hot air oven at 105 °C for 15 min, whereas crystals obtained from other solvents were dried in a desiccator.

2.6. Sulfathiazole in *n*-Propanol System. *2.6.1. Seeded with Linear Cooling Crystallization.* In this crystallization run, the initial solution of sulfathiazole in *n*-propanol was prepared to have a concentration corresponding to a saturation temperature at 60 °C, which is equivalent to a solute concentration at 1.0 g of sulfathiazole per 100 g of 1-propanol. The solubility of sulfathiazole in *n*-propanol is low; for this reason the solute concentration used in this work is considerably dilute compared to typical concentrations used in industry. After all sulfathiazole

(35) Kruger, G. J.; Gafner, G. *Acta Crystallogr.* **1971**, *B27*, 326.

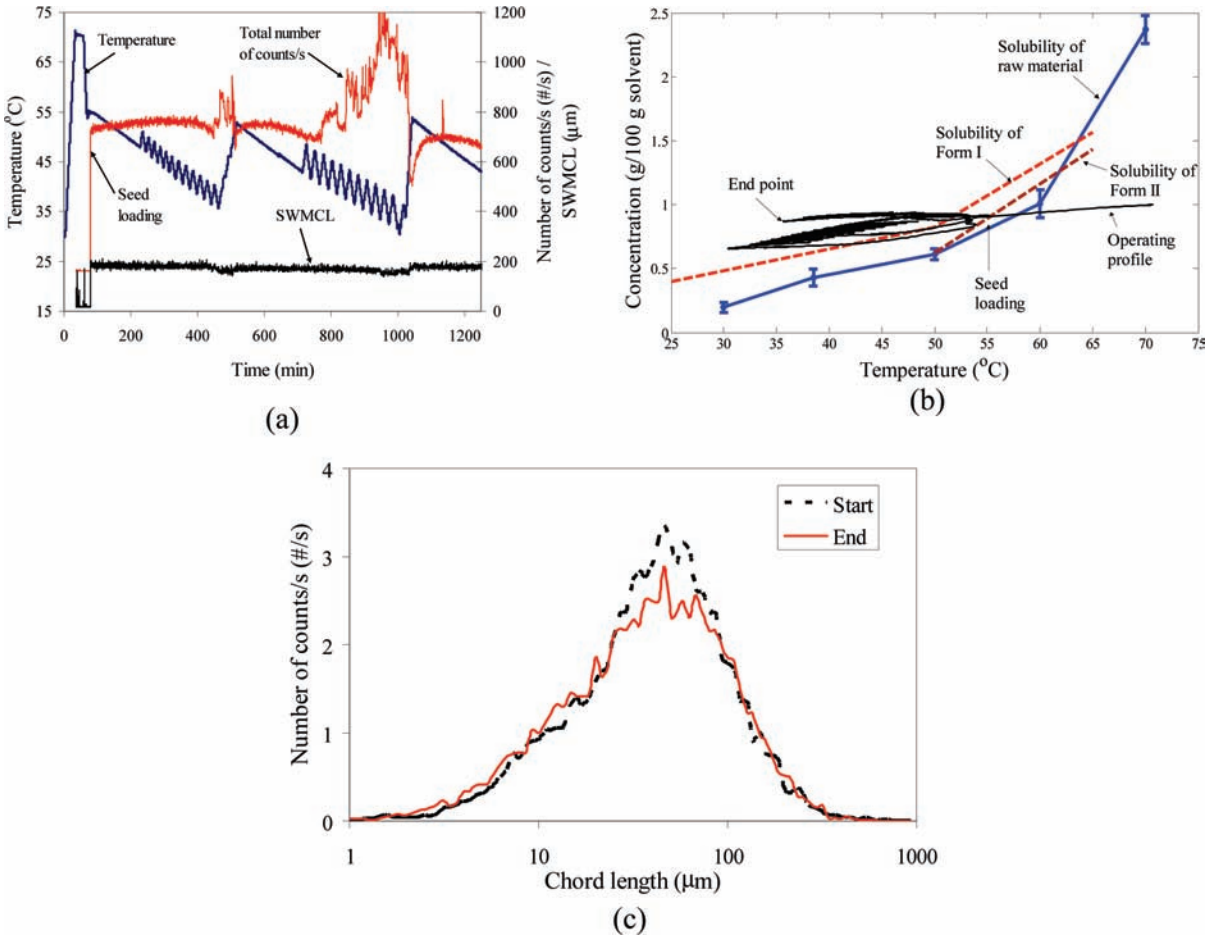

Figure 8. **Profiles of (a) temperature, total number of counts/s and SWMCL; (b) solute concentration on the phase diagram; and (c) CLD at the start and the end of the seeded batch crystallization of Form II in *n*-propanol with temperature cycling.**

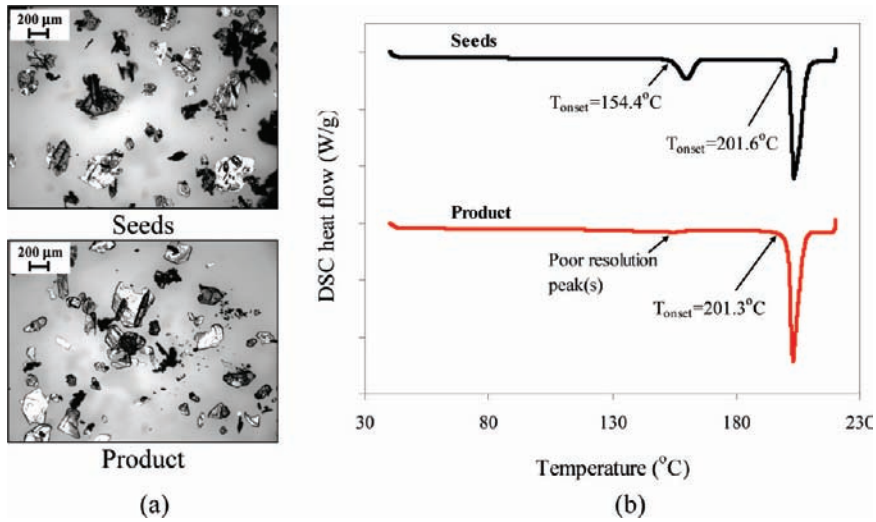

Figure 9. **(a) Microscopy images and (b) DSC curves of the seeds and product of the seeded batch crystallization of Form II in *n*-propanol with temperature cycling.**

crystals were dissolved by heating and maintaining at 70 °C for 15 min, the resultant clear solution was cooled to 55 °C and equilibrated at this temperature before seeds of Form I were loaded. The amount of seeds used was about 10% of the amount of solute in the solution. After the seeds were loaded, the solution was cooled at a slow rate of 0.05 °C/min.

2.6.2. Seeded with Temperature Cycling Crystallization. In this crystallization run, the procedure was the same as in section 2.6.1, but after seeds of Form I were loaded, the system was subjected to temperature cycling with temperature fluctuations between 2 to 4 °C at heating/cooling rates of 1 °C/min, progressively stepping down towards lower temperature. The experiment was repeated with seeds of Form II and Form III.

2.7. Sulfathiazole in Water System. *2.7.1. Seeded Batch with Linear Cooling Crystallization.* The solubility of sulfathiazole in water is lower than in *n*-propanol; for example at 30

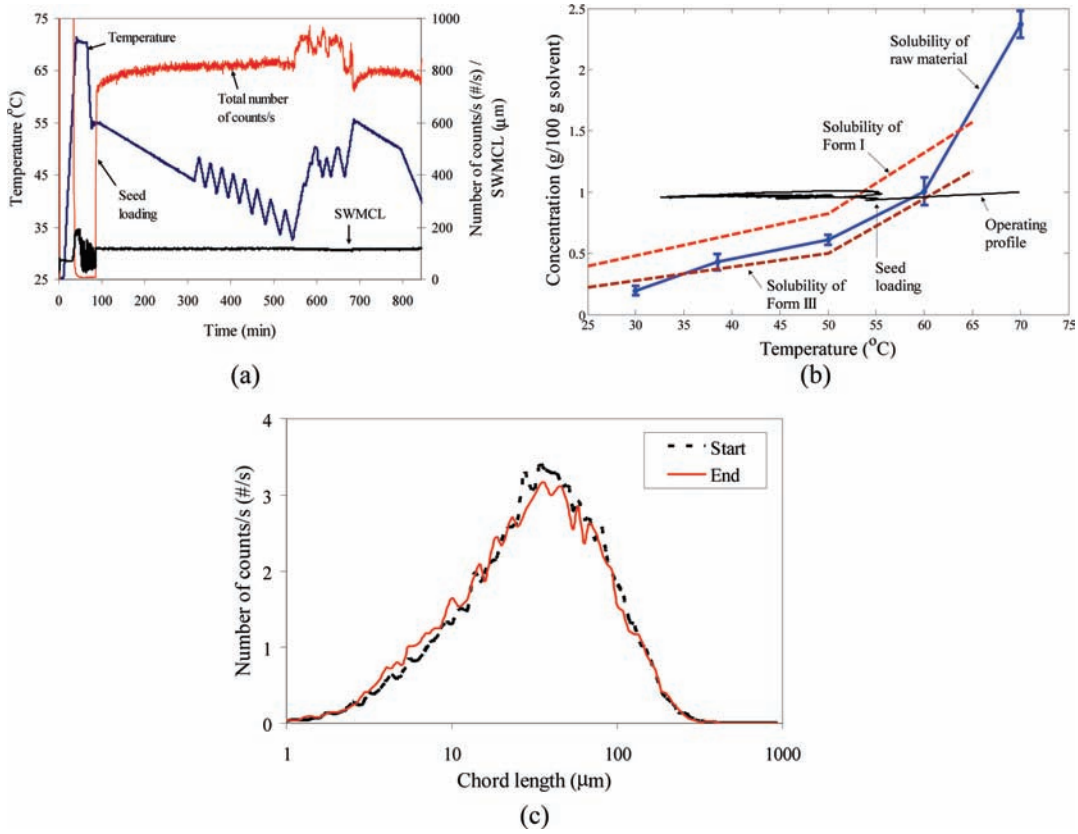

Figure 10. **Profiles of (a) temperature, total number of counts/s and SWMCL; and (b) solution concentration on the phase diagram; and (c) CLD at the start and the end of the seeded batch crystallization of Form III in *n*-propanol with temperature cycling.**

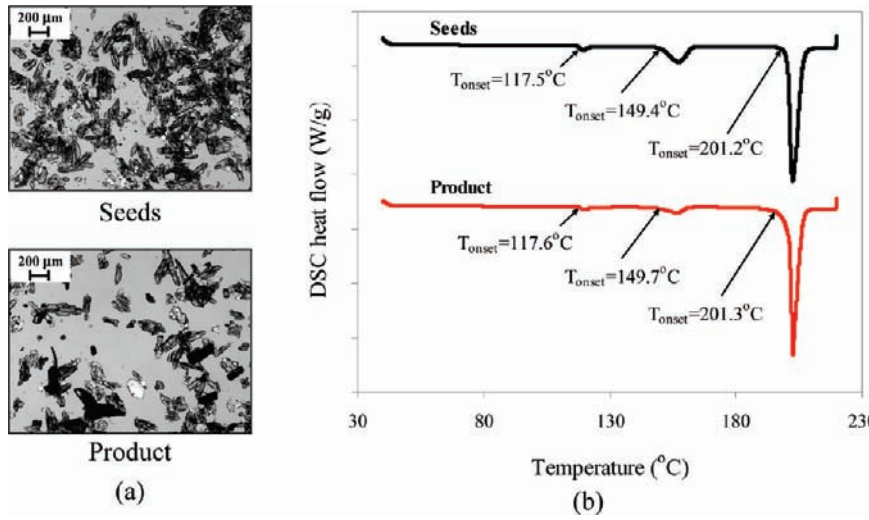

Figure 11. **(a) Microscopy images and (b) DSC curves of the seeds and product of the seeded batch crystallization of Form III in *n*-propanol with temperature cycling.**

°C, the solubilities are 0.1 and 0.2 g per 100 g in water and *n*-propanol, respectively.[33] For a system with lower solubility, the initial solution was prepared to have a concentration corresponding to a higher saturation temperature, in this case at 80 °C (i.e., 1.0 g of sulfathiazole per 100 g of water). After it was heated to complete dissolution, the resultant clear solution was cooled to 78 °C and equilibrated at this temperature prior to the loading of Form II seeds. The same amount of seeds as in previous experiments was used (i.e., 10% of the amount of solute). After the seeds were loaded, the solution was cooled at a linear rate of 0.03 °C/min to 20 °C.

2.7.2. Seeded Batch with Temperature Cycling Crystallization. The procedure was the same as in section 2.7.1, but after the seeds of Form II were loaded, the system was subjected to temperature cycling with temperature fluctuations between 6 to 8 °C at heating/cooling rates of 0.5 °C/min, progressively stepping down towards 20 °C. At the end of the run, the crystals were vacuum filtered and dried for characterization. The experiment was repeated with seeds of Form I.

2.8. Characterization of Crystal Properties. The obtained crystals were characterized for their size uniformity and

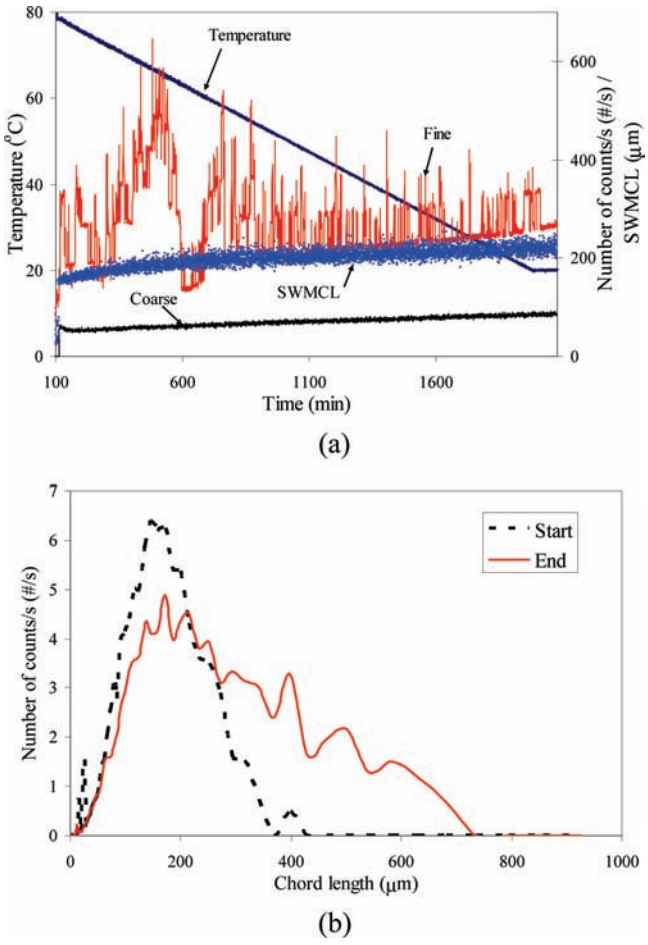

Figure 12. **Profiles of (a) temperature, fine, coarse and SWMCL; and (b) CLD at the start and the end of the seeded batch crystallization of Form II in water with linear cooling.**

polymorphic form using optical microscopy and differential scanning calorimetry (DSC), respectively.

Optical microscopy - the crystals were visually examined using a Leica DMLM optical microscope, and their images were captured and processed using Leica QWin software (version 3.0, Leica Microsystems Digital Imaging).

DSC - the thermal behaviour of the crystals was examined using a TA Instruments Q10. About 8 mg of crystals was weighed into an aluminium pan and sealed hermetically. Analysis was carried out by heating the sample from 40 to 220 °C at a heating rate of 10 °C/min under constant purging of nitrogen at 40 mL/min. An empty aluminium pan was used as a reference in all the runs.

3. Results and Discussion

3.1. Calibration Model. Temperature and the absorbance spectra at the highest peak, 291 nm as marked by a dashed line in Figure 3a, were correlated with the sulfathiazole concentration. Analysis of the calibration data showed that the effect of temperature on the absorbance was linear for a given concentration, however the slopes increased with increasing concentration, indicating the need for an overall nonlinear calibration model. Standard linear robust chemometrics approaches (e.g., based on partial least-squares or principal component regression) do not work in this case, hence a simple nonlinear function was used for the calibration,

$$C = p(1)T + p(2)A + p(3)AT + p(4) \qquad (1)$$

where C denotes solution concentration, T represents temperature (in °C), and A represents absorbance at 291 nm. The parameters of the calibration model, $p(1)$, $p(2)$, $p(3)$ and $p(4)$, were computed as 0.0006, 14.8480, 0.1509 and −0.0618, respectively, through least-squares optimization implemented in Matlab using the *fmincon* function, by minimizing the sum-square errors between the experimental concentrations and the concentrations obtained from eq 1. The value of the minimized sum-square error is 0.0016.

As shown in Figure 3b, the difference between experimental and simulated concentrations using the calibration model is very small, and the maximum error was calculated to be less than 5%, judging from the two validation points, which were not part of the data set used to obtain the parameters in eq 1. In the subsequent analysis of this work, eq 1 was used as a calibration to relate temperature and absorbance spectra to the sulfathiazole concentration.

3.2. Sulfathiazole in *n*-Propanol System. *3.2.1. Seeded Batch with Linear Cooling Crystallization.* Figure 4a shows the profile of temperature and the evolutions of fine and coarse crystals and the square-weighted mean chord length (SWMCL) during crystallization. Fines were defined to be crystals with chord lengths of <20 μm, whereas coarse were defined to be crystals with chord lengths of >100 μm. The SWMCL statistic was found to resemble more closely the Sauter mean diameter measured using a laser diffraction instrument[36,37] and optical microscopy.[37,38] Although the FBRM data do not correspond quantitatively to laser diffraction or optical microscopic data (since they are based on different principles of measurement), the trends can be analysed to give information about the dynamic progress of the crystallization process.

With reference to Figure 4a, it can be seen that about 30 min after seed loading, the number of fines reduced until it stabilized approximately 60 min later. At the same time and over the same period, the number of coarse and SWMCL increased. This indicates the occurrence of Ostwald ripening in which some fine seed crystals dissolved and immediately recrystallized on the surface of the remaining larger crystals. This, however, can also be due to the effect of a morphology change of the seed crystals that affected the FBRM readings—the microscopy images of seed and product, presented later in Figure 7a, show that the product appears to be more platelike, whereas the seed is more rodlike. The crystallisation was stopped after a nucleation event was detected, as indicated by a sudden change in the number of fines at about 44 °C (marked by dashed lines in Figure 4a). Figure 4b shows the solute concentration profile of the crystallization on the phase diagram. The solubility curve of Form I, shown by a dashed line in Figure 4b, was plotted on the basis of literature value,[32] whereas the solubility curve of raw sulfathiazole, shown by a solid line in the same figure, was plotted on the basis of gravimetric analysis

(36) Heath, A. R.; Fawell, P. D.; Bahri, P. A.; Swift, J. D. *Part. Part. Syst. Charact.* **2002**, *19*, 84–95.
(37) Yu, W.; Erickson, K. *Powder Technol.* **2008**, *185*, 24–30.
(38) Chew, J. W.; Black, S. N.; Chow, P. S.; Tan, R. B. H. *Ind. Eng. Chem. Res.* **2007**, *46*, 830–838.

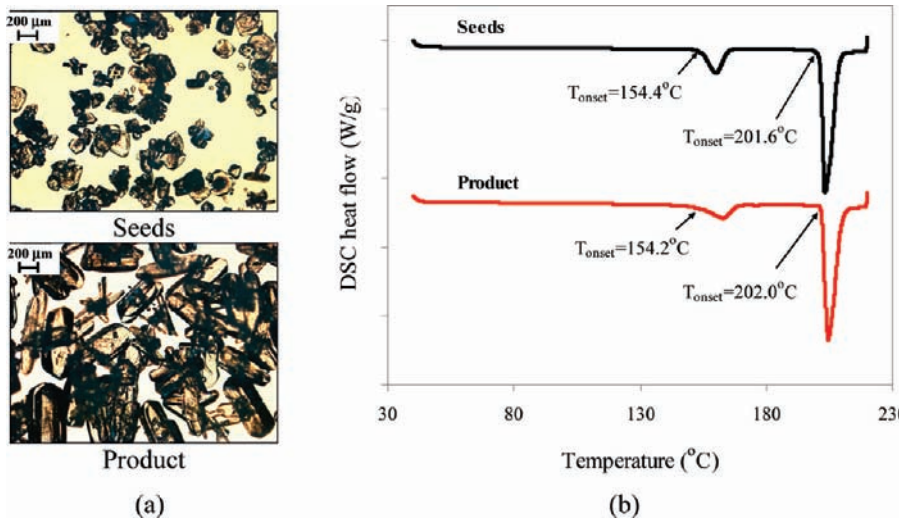

Figure 13. **(a) Microscopy images and (b) DSC curves of the seeds and product of the seeded batch crystallization of Form II in water with linear cooling.**

(see section 2.3). It can be observed that the solute concentration reduced continuously during cooling but remained in the supersaturation region of Form I. This continuous reduction in the solute concentration corresponds very well with the continuous increase of the SWMCL during cooling as shown in Figure 4a, indicating that the seed crystals were continuously growing. This was confirmed by the profiles of the chord length distribution (CLD) during the crystallization run as depicted in Figure 4c, where crystal growth was indicated by slight shift of the CLD for the end product and that for the crystals before the primary nucleation to the right. The occurrence of nucleation towards the end of the run, however, resulted in a bimodality of the end product's CLD.

Microscopy images of the seed and product crystals, shown in Figure 5a, confirmed the inference made on the basis of the profiles of SWMCL, solute concentration and CLD that there was crystal growth. It can also be seen from the images that the product is characterized by more platelike crystals compared to the seed, which appears to have more rodlike crystals. This may be the reason for the change in number of fine, coarse and SWMCL about 30 min after the seed loading, since the FBRM is sensitive to changes in the shape of the monitored particles. The microscopy images also showed that the seed crystals propagated their polydispersed CSD to the end product. This underscores the importance of having a controlled manipulation of temperature after seed loading, to correct for the poor quality of the seed crystals. The DSC curves of the seed crystals and the product in Figure 5b show the presence of single peaks, with onsets at 201.0 and 200.8 °C, respectively. These DSC curves are the characteristic of Form I crystals. The results indicate that both seed crystals and product were pure Form I.

3.2.2. Seeded Batch with Temperature Cycling Crystallization. 3.2.2.1. Seeding with Form I. The profiles of temperature, total number of counts/s and SWMCL during crystallization run are presented in Figure 6a. The total number of counts/s represents a total number of crystals with a chord length range from 1 to 1000 μm and is sensitive to changes in fines since crystals with the fine size range are predominant. It can be seen that the evolutions of total number of counts/s and SWMCL for the first 200 min after seed loading are very similar to the profiles in section 3.2.1. This indicates the consistency of the occurrence of Ostwald ripening. Temperature cycling was started when the temperature of the suspension reached 48 °C. This temperature was chosen on the basis of the onset of nucleation in the previous crystallization run. However, as can be seen in Figure 6a, the nucleation occurred at around 49 °C. Although the temperature cycling was started around 25 min after the nucleation, the total number of counts/s in the system has successfully been brought as close as possible to the initial number of seed crystals. During the implementation of temperature cycling, the amplitudes of temperature change were varied accordingly (between 2 to 7 °C) in order to keep approximately the same number of counts/s in the system, whilst the heating/cooling rates were maintained at 1 °C/min. It can be seen in Figure 6a that the overall trend of the total number of counts/s is increasing. This is probably due to the nature of Form I crystals; they tend to grow in elongated form, which subsequently were broken, and consequently the total number of counts/s increased. The profile of the solute concentration on the phase diagram in Figure 6b follows the hypothetical operating profile very well. The continuous growth of the crystals in the system can be inferred from the increasing trend of the SWMCL profile in Figure 6a and the decreasing trend of the solute concentration in Figure 6b. The profiles of the CLD at the start and at the end of the crystallization run, as shown in Figure 6c, also indicate crystal growth since the CLD at the end of the run is slightly shifted to the right of the CLD at the start, after the seed was introduced in the system.

The growth of the crystallization product inferred by the profiles of SWMCL and solute concentration was confirmed visually by microscopy images as shown in Figure 7a. The images also show the improvement of size uniformity in comparison to the seed crystals. The DSC curves in Figure 7b show that the seed crystals of Form I have grown into the same polymorphic form.

3.2.2.2. Seeding with Form II. The profiles of temperature, total number of counts/s and SWMCL during seeded batch cooling crystallization of Form II with temperature cycling are

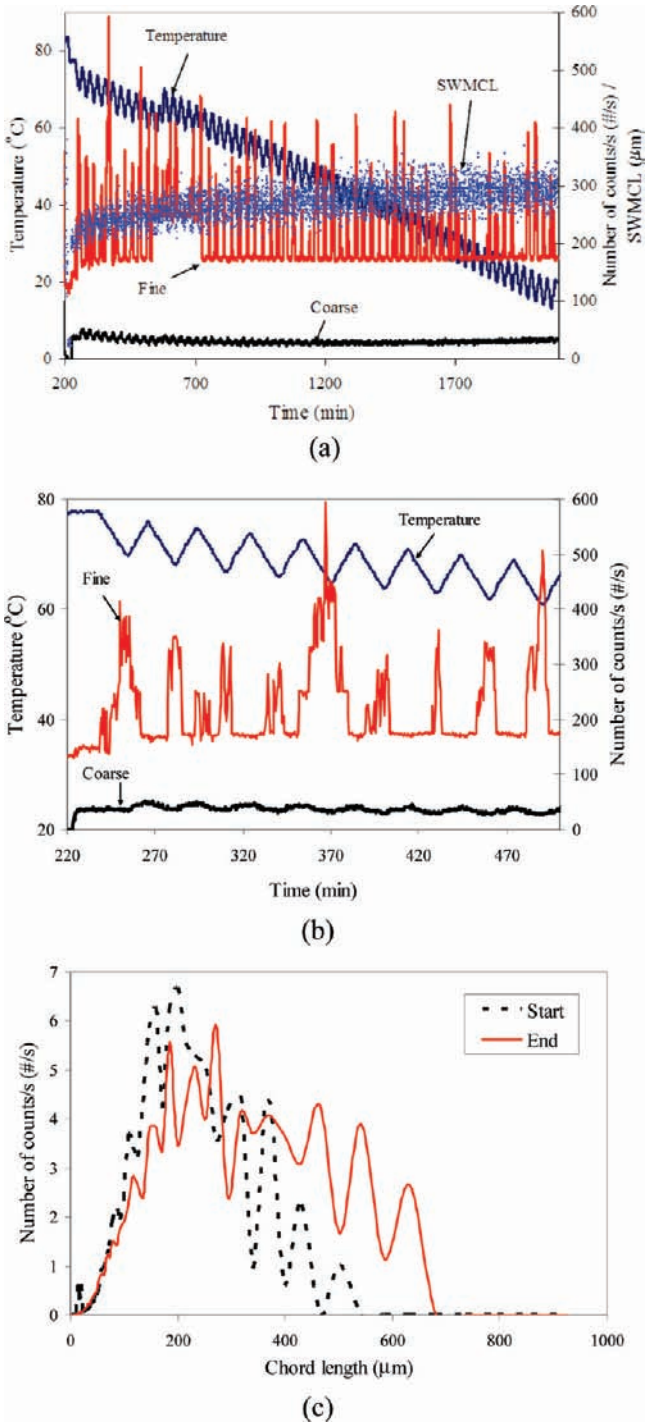

Figure 14. **(a) Profiles of temperature, fine, coarse and SWMCL; (b) zoom-out view of a part of the profiles of fine, coarse and temperature; (c) profiles of CLD at the start and the end of the seeded batch crystallization of Form II in water with temperature cycling.**

shown in Figure 8a. Unlike in the previous crystallization run, no drop in the total number of counts/s was observed within the first 200 min after seed addition. The seed crystals were suspended in the solution without showing any growth for about 5 h. The temperature cycling was started when the suspension reached 48 °C and continued through to 36 °C with temperature fluctuations of 2 °C and heating/cooling rates of 1 °C/min. The total number of counts/s showed a sudden increase when the suspension reached 39 °C, which indicates the occurrence of nucleation. At the same time, the SWMCL showed a slight drop, which is influenced by the presence of fine crystals (nuclei). In order to eliminate the newly formed fine crystals and maintain the number of seed crystals, the suspension was heated to 53 °C. Once the total number of counts/s returned to the initial value, the suspension was subjected to a slow cooling at 0.05 °C/min. The temperature cycling was started again when the suspension reached 43 °C and continued through to 30 °C with temperature fluctuations of 4 °C and heating/cooling rates of 1 °C/min. The total number of counts/s showed a sudden increase again at 42 °C, which indicates the start of another nucleation. The presence of polymorphic impurities produced from the previous nucleation may act as seeds which results in the earlier occurrence of nucleation. Although the temperature cycling was implemented, the heating phases were not able to bring the total number of counts/s back to the initial value, and for this reason, when the total number of counts/s exceeded 1000 counts/s, the suspension was heated to 53 °C. This time the heating was too much, and the total number of counts/s dropped to below the initial value. Immediately, the suspension was cooled linearly, and in the process, the total number of counts/s increased to slightly below the initial value. The run was stopped at 43 °C to avoid another nucleation. Other than showing slight decreases when nucleation events were detected, the profile of the SWMCL was generally flat during the run, which indicates no crystal growth. Figure 8b shows the operating profile of the crystallization run on the phase diagram. The solubility curve of Form II in the figure was plotted according to literature data.[32] It can be seen from the figure that the crystallization run was operated in the supersaturated regions of both Form I and Form II. The operating profile showed a decreasing trend in concentration due to the formation of nuclei during the nucleation events but returned close to the initial concentration towards the end due to the dissolution of the nuclei as shown in Figure 8b. The inability of the Form II crystals to grow was also shown by the almost overlapping profiles of the CLD at the start and the end of the crystallization run in Figure 8c.

No size change between the seed crystals and the product was visually observed on the basis of the microscopy images in Figure 9a. This confirmed the result inferred from the profiles of SWMCL and CLD. The DSC curve of the seed crystals shown in Figure 9b has two peaks; one at 154.4 °C and another at 201.6 °C, which is a characteristic DSC curve for Form II crystals. The DSC curve of the product, on the other hand, shows the presence of a major peak at an onset temperature of 201.3 °C and poor resolution peak(s) that lie between 140 to 160 °C. The difference between the DSC curves of the seed and the product indicates that the crystals produced by the nucleation events have contaminated the seed crystals. Nucleation is thought to produce Form I crystals because the intensity of the transition peaks of Form II were swamped by the melting peak of Form I. It was reported that Form I always crystallizes from *n*-propanol, and although it is the least stable form in the solvent, it did not transform to other forms even after a month of storage as slurry at 30 °C.[39] Above the nucleation temperature, seeds of Form II are expected to stay as Form II without

(39) Blagden, N.; Davey, R. J.; Lieberman, H. F.; Williams, L.; Payne, R.; Roberts, R.; Rowe, R.; Docherty, R. *J. Chem. Soc., Faraday Trans.* **1998**, *94* (8), 1035–1044.

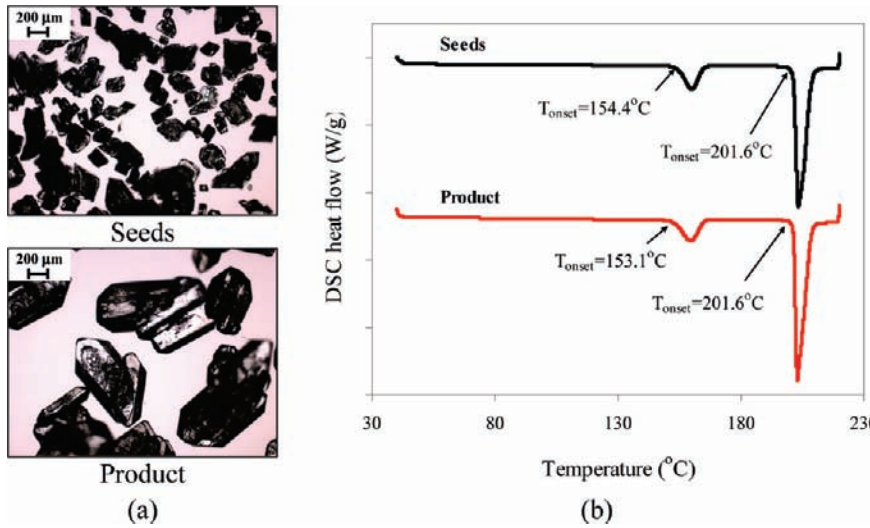

Figure 15. **(a) Microscopy images and (b) DSC curves of the seeds and product of the seeded batch crystallization of Form II in water with temperature cycling.**

transformation because it is more stable than Form I in *n*-propanol as can be inferred from the position of their solubility curves in Figure 8b.

Sudo and co-workers[40] made the same observation, in which seed crystals of one polymorph did not grow, but instead the system nucleated another polymorphic form. In their work on the crystallization of cimetidine, they found that one of its polymorphic forms, which is a thermodynamically metastable form in IPA solution, was crystallized from highly supersaturated IPA solution with or without seed and regardless of the polymorphic form of seed.

3.2.2.3. Seeding with Form III. Figure 10a depicts the profiles of temperature, total number of counts/s and SWMCL during seeded batch cooling crystallization of Form III with temperature cycling. The temperature cycling with amplitudes between 5 to 7 °C and heating/cooling rates of 1 °C/min was started when the temperature of the suspension reached 44 °C and continued until the total number of counts/s started to increase at approximately 33 °C. In order to suppress the nucleation and return the total number of counts/s to the initial value, the suspension was then heated to 50 °C at a rate of 1 °C/min. Thereafter a couple of cycles with maximum temperatures of 48 and 50 °C were applied, but since this was still unable to reduce the total number of counts/s, the suspension was further heated to 55 °C, the same temperature as was used for the initial seed loading. The heating reduced the total number of counts/s to below the initial value, but the cooling process performed after that brought the total number of counts/s closer to the initial value. The cooling was conducted at two rates; 0.05 °C/min from 55 to 50 °C, and 0.10 °C/min from 50 °C and below. The crystallization run was stopped at 40 °C in order to avoid a nucleation event that may affect the quality of the product. It can be seen from Figure 10a that after the seed loading, the profile of SWMCL was completely flat, which indicates no crystal growth. The same can be inferred from the profile of solute concentration on the phase diagram in Figure 10b, which shows the system stayed in the supersaturated region without any significant change in the solute concentration. Figure 10c shows profiles of the CLD at the start and at the end of the crystallization run that are almost overlapped, which also indicates the absence of crystal growth.

Microscopy images in Figure 11a show that there was no significant different in size between seed and product crystals. This confirmed the result inferred from the profiles of SWMCL and CLD and also confirmed a similar behaviour of the sulfathiazole in *n*-propanol system to cimetidine in IPA, as mentioned in the previous section. It can also be seen from the microscopy images that the product appears to have fewer fine particles than the seed, which may be due to the effect of the temperature cycling. The DSC curve of seed crystals shown in Figure 11b is consistent with the one reported in our previous work[21] and is characteristic for Form III crystals. The product crystals have all the same peaks as the seed crystals, but with lower intensity. This may be due to a slight contamination of seed crystals with the product of nucleation. Regardless of the contamination, this result implies the prospect of the temperature cycling method in controlling polymorphic purity of the end product.

3.3. Sulfathiazole in Water System. *3.3.1. Seeded Batch with Linear Cooling Crystallization.* Figure 12a shows the profile of temperature and the evolutions of the number of fine and coarse crystals, and the SWMCL for the seeded batch crystallization of Form II in water with linear cooling. During cooling after seed loading at 100 min, the number of fines continuously fluctuated due to nucleation and dissolution events. The nucleation events kept producing fine particles, and as a result, the trend of the overall profile of the fine particles increases. The profiles of numbers of counts/s of coarse particles and the SWMCL also show a continuous increase, which indicates a continuous growth of the crystals present in the system. The difference in the profiles of the CLDs at the start and at the end of the experimental run as shown in Figure 12b provides further evidence of the crystal growth.

The nucleation and growth events inferred from the profiles of fine, coarse, SWMCL and CLD are confirmed by the microscopy images in Figure 13a. The microscopy images show

(40) Sudo, S.; Sato, R.; Harano, Y; Ogo, Y. *Chem. Eng. Jpn.* **1991**, *24*, 237–242.

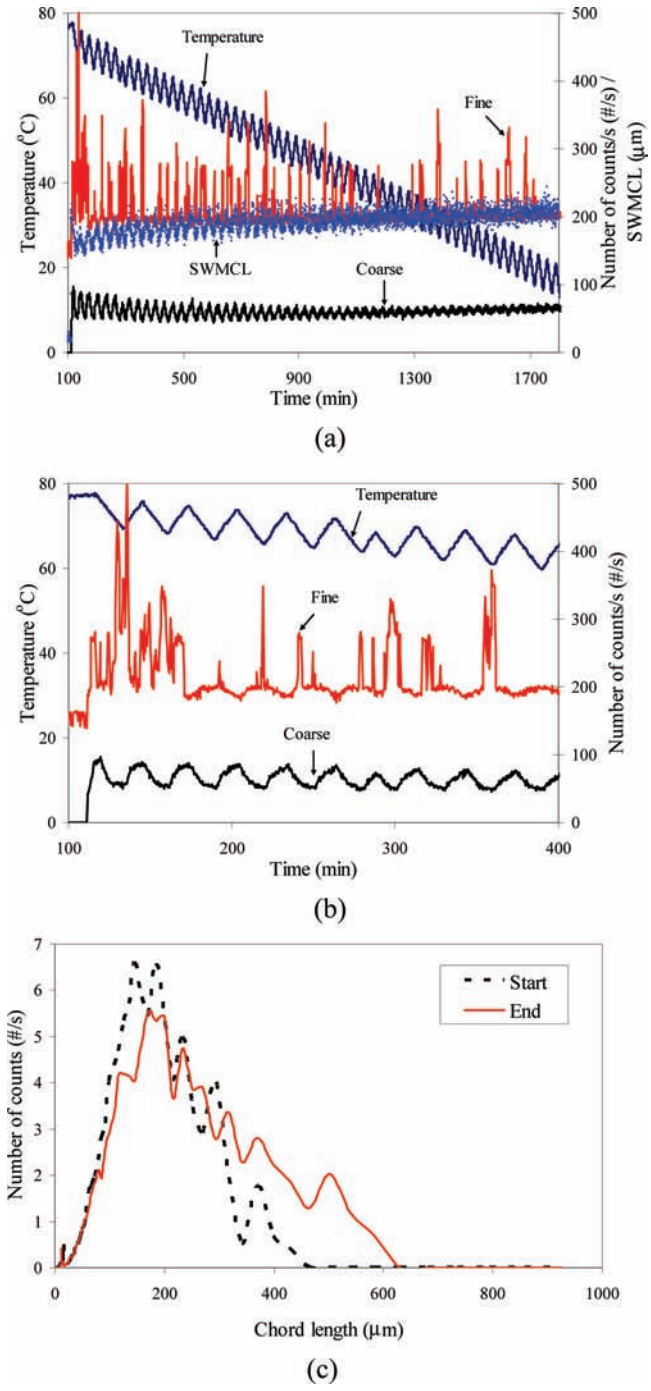

Figure 16. **(a) Profiles of temperature, fine, coarse and SWMCL; (b) zoom-out view of a part of the profiles of fine, coarse and temperature; (c) profiles of CLD at the start and the end of the seeded batch crystallization of Form I in water with temperature cycling.**

that there is a significant difference in size between seed and product crystals, which indicates growth. The image of the product shows the presence of much smaller crystals among the larger ones. These smaller crystals are most likely the products of nucleation events that had occurred during the cooling process. This shows that besides correcting the effects of poor quality of the seed crystals, as shown in section 3.2.1, a controlled manipulation of temperature after seed loading is necessary to prevent unwanted nucleation, or in cases where nucleation cannot be prevented, to eliminate nuclei so that they could not contribute to the poor size uniformity of the end product. DSC curves presented in Figure 13b show that seeds and product are of the same polymorph. It can be confirmed from the results of microscopy and DSC analyses that water is the preferred solvent for Form II crystals to grow as well as to nucleate, whereas in *n*-propanol (preferred solvent for Form I) the Form II seeds do not grow at all.

3.3.2. Seeded Batch with Temperature Cycling Crystallization. 3.3.2.1. Seeding with Form II. The profiles of temperature, number of fine, number of coarse and SWMCL during seeded batch cooling crystallization of Form II with temperature cycling in water are shown in Figure 14a. The figure shows that the number of fines fluctuated with the change in temperature due to nucleation and dissolution events while maintaining almost the same number of counts/s throughout the batch. The number of coarse particles was similarly fluctuating and as can be seen more clearly from a zoom-out view of a part of the profiles of fine, coarse and temperature in Figure 14b, the number of fine and coarse responded to temperature change out of phase with each other: on heating, the number of fine dropped while the number of coarse increased, whereas on cooling, the fines increased while the coarse reduced. These responses of fine and coarse to temperature change evidently indicate the occurrence of Ostwald ripening. Since the temperature fluctuations increase the kinetics of Ostwald ripening, the application of temperature cycling after seed loading is a beneficial method to accelerate the growth of crystals and to eliminate the fine particles. Figure 14a also shows that the amplitude of the fluctuations of coarse reduces with time. It can also be observed that the first half of the coarse profile shows a decreasing trend, while on the second half it shows an increasing trend. These observations may be due to a transition of the crystallization process from a nucleation dominated to a growth dominated process. The profile of the SWMCL in Figure 14a shows a continuous increase, which indicates a continuous growth of the crystals in the system. The difference between the CLDs at the start and at the end of the batch presented in Figure 14c provides further evidence of the crystal growth.

The growth of the crystals in the system is confirmed visually on the basis of the microscopy images in Figure 15a. The images clearly show that the product crystals are much larger in size compared to the seed crystals. The DSC curves in Figure 15b confirmed that the seeds and product are the same polymorph. This is to be expected since water is the preferred solvent for Form II. An inspection of the images for visual comparison of the product of linear cooling (Figure 13a) and the product of temperature cycling (Figure 15a) shows that, besides improving the size uniformity, the temperature cycling method also increases the size of the crystals. As can be determined from Figure 12a and Figure 14a, the average SWMCL at the end of the batch is 220 μm for the linear cooling and 300 μm for the temperature cycling.

3.3.2.2. Seeding with Form I. Figure 16a depicts the profiles of temperature, fine, coarse and SWMCL during seeded batch crystallization of Form I in water with

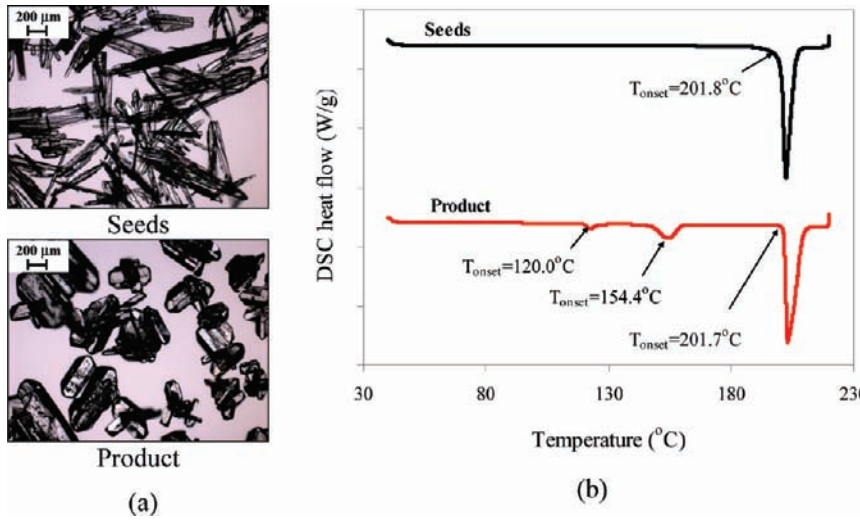

Figure 17. **(a) Microscopy images and (b) DSC curves of the seeds and product of the seeded batch crystallization of Form I in water with temperature cycling.**

temperature cycling. It can be seen that the fine and coarse particle counts also show fluctuations throughout the batch time. As Figure 16b shows, the fine and coarse particles responded to temperature change in reverse of each other. This provides evidence for the occurrence of Ostwald ripening. Similar to the previous experiment, the amplitude of fluctuations of the coarse is also reduced with time, which indicates a transition from a nucleation-dominated to a growth-dominated process. Although the evolution of SWMCL implies growth, the growth took place after the seeds of Form I transformed into Form II crystals and/or were swamped by the nuclei of Form II (as shown by DSC analysis later). In other words, the growing crystals were Form II and not Form I. Form II is the preferred form in water, a solvent which does not promote the formation of Form I. Therefore, during the initial part of the batch the Form I seed particles cannot grow, they merely serve as initiator particles for the heterogeneous secondary nucleation of Form II particles, yielding to a gradual polymorphic transformation of the Form I seed into From II. After enough Form II has formed, these particles can grow in water, and hence, the process gradually becomes growth dominated. This is indicated by the gradually decreasing amplitude of the FBRM counts in Figure 16a. The growth of the crystals in the system is also shown in Figure 16c by the difference between CLD at the start and CLD at the end of the batch.

Microscopy images in Figure 17a show that, during the process, the rodlike Form I seed crystals turned into crystals with a morphology that is typical of that of Form II. The change in polymorphic form between the seeds and the product is confirmed by the DSC analysis—the curves are shown in Figure 17b. The seeds produced a DSC curve with a single melting peak at the onset temperature of 201.8 °C—a characteristic of Form I crystals, while the product produced a DSC curve with peaks at 154.4 and 201.7 °C—typical DSC peaks for Form II crystals and a small peak at 120 °C—a typical DSC peak due to the formation of hydrate. Water is also present because larger crystals tend to entrap water (solvent) in their structure, and the entrapped water is harder to be removed by a normal drying procedure.

The seeds of Form I in water transformed into Form II because Form I is a metastable polymorph in water and water is a preferred solvent for the crystallization of Form II. Although Form I is a preferred polymorph to crystallize from *n*-propanol, the seeds of Form II did not transform to Form I in *n*-propanol because Form II is a more stable polymorph than Form I in the solvent. As shown in this work, Form I seed crystals grew in *n*-propanol, but not in water. Form II seed crystals on the contrary grew in water, but did not grow in *n*-propanol. Form III seed crystals also did not grow in *n*-propanol. These results are most likely due to the nature of the sulfathiazole polymorphs where their nucleation and growth are dependent very much on solvent. The inability of the seeds of Form II and Form III to grow in *n*-propanol may also be due to the effect of impurities, which originates from the finding of Blagden and co-workers[39,41] who showed that the presence of ethamidosulfathiazole (one of the byproducts of sulfathiazole synthesis) did not disturb the growth of Form I but inhibited the growth of other forms. However, in our work no impurities in the raw material, seeds and products were detected by high performance liquid chromatography (HPLC) method, providing supportive evidence that the observed effects are due to the solvent-mediated nucleation and growth of the sulfathiazole polymorphs. Note that the proposed method of temperature cycling can also be applied for systems with low and flat solubility curves. In these cases the seed loading would be significantly higher than the usual 1−3% of the initial amount used in typical crystallizations, and the role of temperature cycling would be to enhance CSD uniformity by promoting Ostwald ripening, and to selectively dissolve unwanted polymorphs from a mixture, rather than the actual production/separation of a crystalline product from

(41) Blagden, N.; Davey, R. J.; Rowe, R.; Roberts, R. *Int. J. Pharm.* **1998**, *172*, 169–177.

solution, due to the difficulty to achieve practical productivities with reasonable solvent consumptions. The overall trend of the temperature cycles should be tailored in this case to the flat solubility of the system (a much smaller slope or cycling around a constant temperature would be used).

4. Conclusions

Seeded batch cooling crystallization with the temperature cycling method has been implemented using sulfathiazole in *n*-propanol and in water as model systems. Results of the experiments show that the method is capable of accelerating the growth and enhancing the size uniformity of the crystals in comparison with runs using a simple linear temperature profile, by promoting Ostwald ripening. The results also show that the temperature cycling method has a good prospect in the control of polymorphic purity. The inability of the seeds of Form I to grow in water and that of seeds of Form II and Form III to grow in *n*-propanol show that the growth of the systems is solvent mediated. The insights into this behaviour of sulfathiazole crystals were captured very well by FBRM and ATR-UV/vis. In some cases, particularly those that involve polymorphic transformation, the use of in-process video microscopy, such as Mettler Toledo's process vision measurement (PVM), would be useful to provide a complete visual insight during the transformation process and thus help in describing the actual process.

Acknowledgment

Financial support provided by the Engineering and Physical Sciences Research Council (EPSRC), U.K., (Grant EP/E022294/1) is gratefully acknowledged. M.R.A.B. is grateful to the Malaysian Ministry of Higher Education and the International Islamic University Malaysia for a scholarship.

Received for review July 9, 2009.

OP900174B